AFM anodization studied by Spectromicroscopy

M. Lazzarino*,[1], G. Mori*, D. Ercolani*, B. Ressel*, A. Colli*, L. Sorba*,***, A. Locatelli**, S. Cherifi**, A. Ballestrazzi*** and S. Heun**
*Laboratorio Nazionale TASC-INFM, I-34012 Trieste, Italy
**Sincrotrone Trieste S.c.p.a, I-34012 Trieste, Italy
*** Università di Modena e Reggio Emilia, I-41100 Modena, Italy

ABSTRACT

Atomic force microscope (AFM) local oxidation is an innovative nanofabrication technique applied to the fabrication of quantum devices. Nevertheless, little information is available on the chemical and structural properties of the grown oxide. We studied by spatially resolved spectroscopy the chemical properties of Si and GaAs AFM oxides. We found that AFM oxidation produces chemically uniform, stoichiometric oxides in the case of silicon, while different non stoichiometric oxides are produced on GaAs as a function of the writing voltage. Moreover we observed a never reported strong photodesorption effect of As oxide.

Keywords: AFM local anodic oxidation, photodesorbtion, microspectroscopy

1 INTRODUCTION

The fabrication of state-of-the-art semiconductor nanostructures is of great interest both for fundamental physics and device applications. Besides the traditional nanolithography techniques, proximal probe microscopies such as the scanning tunneling microscope (STM) and the atomic force microscope (AFM) have attracted attention as potential new tools for nanofabrication because of their demonstrated ability to image and manipulate matter on the atomic level [1].

One of the most promising techniques that uses AFM and STM is local anodic oxidation (LAO): here the active layer of a semiconductor heterostructure can be directly oxidized to produce nanopatterns or nanodevices [2].

In spite of the ease and the effectiveness of the LAO process, little information is available on the chemical nature of the patterned oxide. Among the literature published on the AFM and STM oxidation processes, only few groups investigated the chemistry of the obtained oxides. Okada reported on the chemical properties of GaAs AFM induced oxide [3] studying an oxide patch of 10μm in size with x-ray photoemission spectroscopy (XPS). However, the signal coming from the oxide was weak compared to that coming from the substrate, and the results shown are not very clear. Klauser et al. used spatially resolved spectroscopy to demonstrate the scanning probe induced conversion of Si_3N_4 in SiO_x. [4]

We present here a spectroscopic analysis on AFM oxidised Si and GaAs.

2 EXPERIMENTAL

The Si and GaAs substrates were n-doped wafers covered with native oxide on which gold markers were deposited by standard lithographic techniques. We did not remove the native oxide, nor clean the sample surface chemically in order to minimize any chemical contamination of the surface. Oxide structures were created by scanning a commercial AFM silicon tip in air in contact mode over the sample surface; the substrate was grounded and the AFM tip bias was varied from -6V to -16V. After the oxidation the height of the oxide lines was measured with the same AFM. The structural uniformity of the oxidation process was verified on different structures. It is important to stress here that the actual oxide thickness is 1.5 times higher than the measured thickness for the Si and 2.5 times higher for the GaAs since part of the growth occurs below the sample surface [5,6].

To perform a chemical analysis on the oxide lines sensitive both to spatial and spectroscopic issues, we took advantage of the performance of the spectroscopic photoemission and low energy electron microscope (SPELEEM) which is operating at the Nanospectroscopy beamline at Elettra, the synchrotron radiation facility in Trieste, Italy. Here an area of variable size (5-30 μm) of the sample is illuminated with highly monochromatized synchrotron radiation. The photon energy can vary between 20 and 1000 eV and we choose to operate at 132 eV to maximize the Si 2p, As 3d, Ga 3d core level signal. To monitor the O1s core level emission in the case of GaAs oxides we set the photon energy to 600eV. Using a parallel imaging system, the photoelectrons are collected, selected in energy, and projected on a phosphorous screen where the original image is recorded by a CCD camera. In each image the gray scale represents the photoelectron intensity at a fixed energy relative to that specific location. For each pixel it is possible to plot the intensity as a function of the energy producing local photoemission spectra. A detailed explanation of the SPELEEM microscope can be found elsewhere [7].

[1] Corresponding author. e-mail: lazzarino@tasc.infm.it

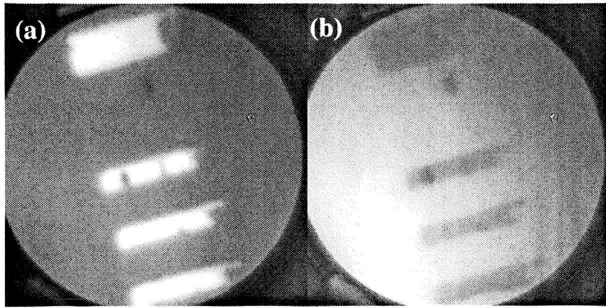

Fig. 1. SPELEEM images around the Si 2p core level. In a) the kinetic energy is slightly lower than the maximum of the peak, in b) it is slightly higher.

3 SILICON

In Fig. 1 we show two selected SPELEEM images obtained at the Si2p core level emission peak. In Fig. 1a) the kinetic energy is slightly lower than the maximum of the peak while in Fig. 1b it is slightly higher. The area represented has a diameter of 12 μm. A strong contrast inversion is observed.

From a complete series of images at different kinetic energies the spectra illustrated in Fig. 2 are obtained. The spectrum represented with a continuous line and symbols refers to an untreated region, covered by native oxide, while the four spectra represented by gray scale continuous lines refers to the four AFM-LAO pattern presented in Fig. 1. The four patterns are produced with different writing voltages, that decrease, from top to bottom, from –14V, –12V, –10V and –8V. Different writing voltages correspond to different thickness, as already reported in literature. Each spectrum is normalized to maximum intensity.

From the spectra in Fig. 2 two peaks are distinguishable. On the right, at minor binding energy, we observe a small peak, with constant energy and relative intensity decreasing with increasing writing voltage and thickness. This peak is related to the emission from the substrate bulk silicon, that is the same for all regions. The different intensity is related to the different attenuation by the differently thick overlayers.

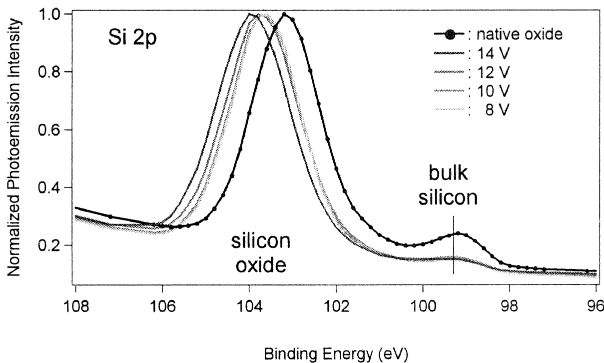

Fig. 2. Si 2p core level spectra: Native oxide (continuous line with dots) and AFM-LAO oxide (continuous gray lines).

The major peaks at higher binding energy are related to the silicon oxide. In the native oxide spectrum, this component is shifted by 3.9 eV with respect to the bulk, as expected for stoichiometric and crystalline SiO_2. The major components from the AFM-LAO oxides have instead a larger shift that increases monotonically with the writing bias, and therefore with the oxide thickness.

We explain this shift in terms of charging of the oxide lines during the photoemission experiments, in agreement with a model proposed by Kobayashi et al. [8]. In the framework of this model a positively charged layer is formed on the oxide surface as electrons are extracted from the sample and positive ions are left inside the oxide. A steady state is immediately reached where the extraction current is compensated by leakage current through the oxide. For higher oxide thickness, the energy shift is higher while the charge density is nearly constant. In our case the surface charge is $Q_s \sim 1x10^{12}$ cm^{-2} and the leakage current is $2x10^{-4}$ Acm^{-2}. In conclusion, we find that the silicon oxide grown by AFM-LAO is stoichiometric, independent of the writing bias, with electrical and structural properties comparable to those of thermally grown oxide [9].

4 GALLIUM ARSENIDE

The case of GaAs is more complicated. Several oxide compounds are reported that involve separately Ga or As atoms or GaAs complexes. We performed both X-ray photoemission spectroscopy (XPS) and synchrotron radiation photoemission spectroscopy (SRPES) in order to take advantage of the different peculiarities of the two techniques. As in XPS we use high energy photons (Al K_α 1486.6eV) we are less sensitive to the surface and we could easily observe the signal from the substrate. On the other hand, spatially resolved SRPES uses low energy photons (132 eV) and is therefore much more surface sensitive.

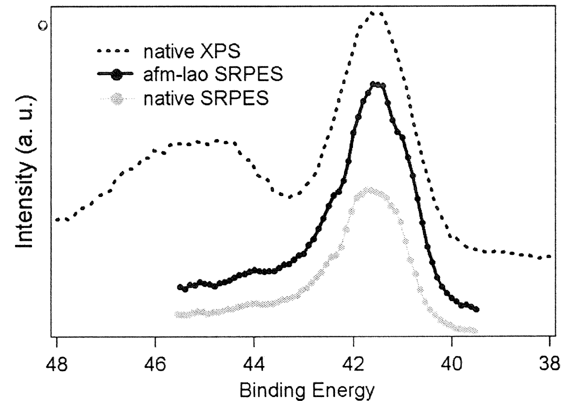

Fig. 3. As 3d core level spectra by XPS (dotted line) on an extended area of native oxide, by spatially resolved SRPES (continuous line - black) on an AFM-LAO structure grown at –12V, and by spatially resolved SRPES (continuous line-gray) on the native oxide.

In the XPS measurements we identified several oxide components on the native oxide, together with the main signal coming from the substrate. In particular, we studied the As3d and Ga3d core level emission peaks. In the As 3d core level spectrum (see Fig. 3) we identified two components related to As_2O_3 and As_2O_5, separated by 3.2 eV and 4.2 eV from the GaAs bulk component, respectively. For the Ga 3d core level spectrum (not shown here) we also identified two components related to Ga_2O and Ga_2O_3, separated by 1.0 eV and 1.6 eV from the GaAs bulk component, respectively.

Surprisingly, by SRPES we observed different features. In Fig. 3 we report the As 3d core level emission peak obtained with the two techniques. The XPS spectrum (top curve) is integrated over a large area far away from the AFM-LAO structures. The SRPES spectra are obtained for the AFM-LAO (intermediate curve) and for the native oxide (lower curve). The GaAs bulk component at 41.5 eV binding energy is clearly evident in all spectra, while the oxide components are present only in the XPS spectrum.

In Fig. 4 we show the SPELEEM images obtained at the Ga 3d (a) and the As 3d core level emission (b). The four square features are the AFM-LAO oxides grown at –16 V (bottom) and at –14 V, –12 V, and –10V (top, from left to right). In Fig. 4a) the Ga intensity appears stronger in the AFM-LAO patterns than in the native oxide for the –16 V and the –14 V squares, but weaker in the two squares at –12 V and –10V. On the contrary, in Fig. 4b) the As intensity appears stronger in the AFM-LAO patterns grown at –10V, –12V, and –14 V, and appears comparable to the native oxide in the –16V square. It seems that the AFM-LAO process *removes* Ga and *adds* As for lower writing voltages, while it *adds* Ga and *removes* As for higher writing voltages.

Moreover, the analysis of the O1s core level images (not shown) reveals that the oxygen concentration, compared to that in the native oxide, is lower for the two low writing voltage patterns, and comparable for the other two.

It is important to stress here that the strong contrast observed in the case of GaAs is different to that observed in the case of Si. In the case of GaAs the intensity contrast is the same for all energies around the core level emission peak, and no contrast inversion is observed. In the case of Si the intensities were comparable, and the contrast was due to an energetic shift of the peak.

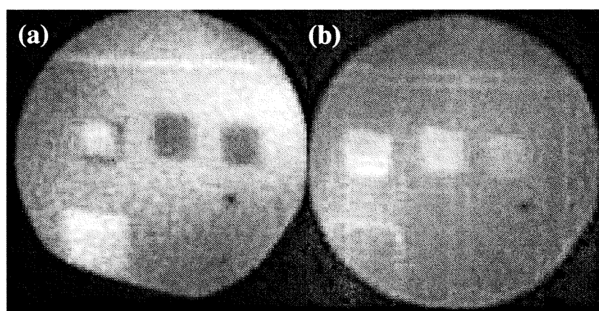

Fig. 4. a) image of the AFM LAO pattern obtained at the Ga 3d core level emission peak. b) Same as in (a) but obtained at the As 3d core level emission peak

We analyzed the As 3d and the Ga 3d core level emission peaks for the four AFM-LAO patterns and for the native oxide close to each pattern. In the case of the As3d the peak shape and position are identical for the four patterns and for the native oxide, with intensity differences already observed by the image analysis. In all cases we did not observe any oxide component as already discussed in Fig. 3, and we attribute the observed peak to As bound in GaAs.

In Fig. 5 we show the Ga 3d spectra for the four AFM-LAO patterns. Each spectrum is plotted together with the corresponding native oxide spectrum obtained from a region close to that of the LAO square. In the case of the –16V and –14V oxides the spectra are comparable with those of native oxide. The spectra are asymmetric and peaked at 19.7 eV of binding energy as a result of the contributions of the GaAs bulk component (19.1 eV) and the Ga_2O component (20.1 eV). The contribution arising from Ga_2O_3 and $Ga(OH)_3$ as well as those arising from metallic Ga are negligible. Details on the peak analysis will be published elsewhere [10].

In the case of the –12V and –10V oxides we observe a shift with respect to the native oxide and a change in the peak line shape, due to an increased contribution of the GaAs bulk component. Here the Ga 3d core level peaks show essentially only the GaAs bulk contribution with a weak shoulder attributed to the Ga_2O oxide. This is in agreement with the decreasing intensity of the oxygen core

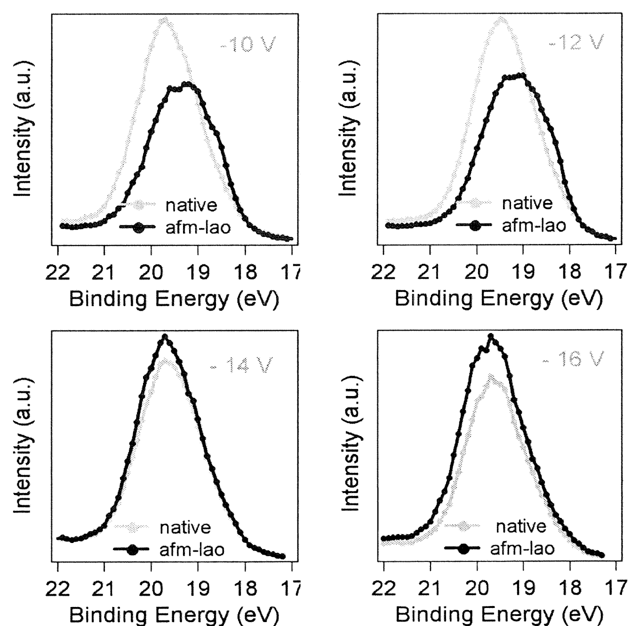

Fig. 5. Ga 3d core level spectra for the AFM-LAO patterns grown at –10V, –12V, –14V, and –16V (black lines) and the corresponding spectra obtained on the native GaAs oxide (gray lines).

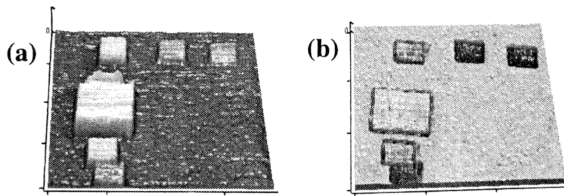

Figure 6: AFM images of the AFM LA oxide just after growth (a) and after synchrotron radiation exposure (b)

level peak emission from the same patterns (not shown).

The spectroscopic results are rather astonishing because a) similar techniques (XPS and SRPES) give contrasting results, and b) the oxide grown by AFM-LAO in some cases contains less oxygen and shows a more intense GaAs bulk component than the native oxide.

In Fig. 6 we compare the AFM topography of the AFM-LAO pattern before (a) and after (b) the SPELEEM measurement. The structures are the same as in Fig. 4.

After exposure to the synchrotron light the oxide patterns' height is strongly reduced and for the patterns grown at lower writing voltage we observed the formation of a hole. We can exclude the possibility of a thermal oxide desorption due to sample heating during the measurement because in several experiments performed at the same beamline and under the same conditions, structures unstable above 100°C were still observed even after days of exposure [11]. We propose therefore that the oxide is partially *photodesorbed* during the SPELEEM measurements. Furthermore, we observed that the desorption of the oxide is a fast process. The structures reported in Fig. 4 were measured immediately after the start of exposure and did not show any further change during time within several hours.

Photon assisted desorption was reported for many systems, generally for atoms or molecules adsorbed on clean surfaces. Some evidence of photodesorption of oxides is reported for SiO_2 and Zirconia [12], but, as far as we know, photodesorption of GaAs oxide has never been reported in literature. In the case of SiO_2 a 1nm thick layer of native oxide was desorbed in 2 hours with a non monochromatized photon density of $1.2x10^{16}$ ph/cm^2, while keeping the substrate at 700°C [13]. The effect we observed is much stronger than what was previously reported in literature and can be partially explained by the much more intense photon density ($5x10^{18}$ ph/cm^2 monochromatized at 132eV), and by the lower stability of GaAs oxide. Recently, the various stages of GaAs oxide thermal desorption have been carefully characterized; it has been reported that AsO desorbs at 150°C; As_2O_3 desorbs at around 300°C; Ga_2O at 400°C, and Ga_2O_3 at 530°C [14].

To explain the observed results we suggest that the mechanisms responsible for the oxide growth in the AFM-LAO process is controlled by the electric field between the AFM tip and the substrate. At high electric field i.e. at high bias a stable Ga_2O is grown. When, as the oxide grows in thickness, the electric field is lowered, a less stable AsO is grown. At lower bias, the electric field is already too low and only AsO is grown. In this case, we photodesorbed all the oxide and we were able to observe the clean substrate. In all cases the electric field was too low to produce more stable (and more oxygenated) oxides such as Ga_2O_3 and As_2O_3.

Further investigation such as micro auger spectroscopy and SPELEEM on high electric field oxides should be performed in order to confirm our hypothesis.

5 CONCLUSIONS

We studied the chemical and structural properties of oxides grown by AFM-LAO on Si and GaAs. In the case of Si we demonstrated that this techniques produces stoichiometric oxide of excellent quality, comparable with those of thermal oxides. In the case of GaAs we observed a photodesorption effect of the arsenic-related oxide and we report a different chemical composition with respect to native oxide. Here we propose an electric field dependent mechanism for the AFM-LAO growth that can explain the observed features.

REFERENCES

[1] D. M. Eigler and E. K. Schweizer, Nature **344**, 524 (1990).

[2] A. Fuhrer, S. Lüscher, T. Ihn, T. Heinzel, K. Ensslin, W. Wegscheider, M. Bichler Nature **413**, 822 (2001)

[3] Y. Okada, Y. Iuchi, M. Kwabe and J.S. Harris J. Appl. Phys **88** 1136 (2000)

[4] R. Klauser, I.H. Hong, H. J. Su, T.T. Chen S. Gwo, S.C. Wang T.J. Chuang and V. A. Gritsenko Appl. Phys. Lett. **79** 3143 (2001)

[5] F. Pérez-Murano, K. Birkelund, K. Morimoto and J. A. Dagata Appl. Phys. Lett. **75**, 199, (1999)

[6] Y. Okada, S. Amano, M. Kawabe and J. S. Harris J. Appl. Phys. 83 7998 (1998)

[7] S. Heun, Th. Schmidt, B. Ressel, E. Bauer, and K. C. Prince, Synchrotron Radiation News, Vol. 12, No. 5 (1999), p.25. See also www.elettra.trieste.it/ /experiments/beamlines/nano/index.html

[8] H. Kobayashi, T. Kubota, H. Kawa, Y. Nakato and M. Nishiyama Appl. Phys. Lett. **73,** 933 (1998)

[9] M. Lazzarino, S. Heun, B. Ressel, K.C. Prince, P. Pingue and C. Ascoli Appl. Phys. Lett. **81**, 2842 (2002)

[10] M. Lazzarino *et al.* to be published

[11] A. Ballestrazzi *et al.* to be published

[12] W. C. Simpson, W. K. Wang, J. A. Yarmoff and T. M. Orlando Surf. Sci. **423** 225 (1999)

[13] T. Miyamae, H. Uchida, I. H. Munro and T. Urisu Surf. Sci. **43**7, L755 (19999)

[14] A. Guillen-Cervantes, Z. Rivera-Alvarez, M. Lopez-Lopez, E. Lopez-Luna and I. Hernadez-Calderon Thin Solid Films. **373**, 159 (2000)